buildings

MDPI

Article

Improving Tunnel Boring Machine Tunneling Performance by Investigating the Particle Size Distribution of Rock Chips and Cutter Consumption

Wei Wang [1], Changbin Yan [2,*], Jing Guo [2], Hailei Zhao [3], Gaoliu Li [4], Wenmin Yao [2] and Taozhe Ren [1]

[1] Pumped-Storage Technological & Economic Research Institute of State Grid Xinyuan Co., Ltd., Beijing 100052, China; wei-wang.jszx@sgxy.sgcc.com.cn (W.W.); taozhe-ren.jszx@sgxy.sgcc.com.cn (T.R.)
[2] School of Civil Engineering, Zhengzhou University, Zhengzhou 450001, China; guojingms@gs.zzu.edu.cn (J.G.); wmyao@zzu.edu.cn (W.Y.)
[3] State Key Laboratory of Shield Machine and Boring Technology, Zhengzhou 450001, China; zhaohailei3@crecg.com
[4] SGIDI Engineering Consulting (Group) Co., Ltd., Shanghai 200093, China; 202022212014093@gs.zzu.edu.cn
* Correspondence: yanchangbin@zzu.edu.cn

Abstract: The construction environment of deep rock tunnels is complex, and effectively enhancing tunnel boring machine (TBM) tunneling efficiency is paramount. Increasing rock-breaking efficiency and minimizing cutter consumption are essential strategies for improving TBM tunneling efficiency. Selecting suitable tunneling parameters is crucial for enhancing rock-breaking efficiency and reducing cutter consumption. Existing research on the optimization of the ratio of maximum cutter spacing to penetration (S_{max}/P) based on field-measured data is limited, and few studies compare and analyze the relationship between *SE*, *CI*, and the S_{max}/P ratio separately. Consequently, this study determined optimal tunneling parameters for various types of surrounding rock and construction environments, aiming to more accurately optimize TBM tunneling performance during construction processes based on on-site construction data. This study conducted a comparative analysis of specific energy (*SE*) and the coarseness index (*CI*). Under both working conditions, the quadratic fitting coefficients of the *CI* are 4.2% and 10.6% higher than those of the *SE*, respectively, with the *CI* selected to represent the particle size distribution of rock chips. Finally, taking into account both the correlations between the *CI* and the ratio of maximum cutter spacing to penetration (S_{max}/P), as well as cutter consumption and the S_{max}/P ratio, an optimization method for the TBM tunneling parameter was established under both dry and saturated conditions. The research findings indicate that cutter consumption exhibits an exponential increase with a higher rock Cerchar Abrasivity Index (*CAI*); it initially decreases as the S_{max}/P ratio increases and subsequently increases in both dry and saturated conditions. Instead, the *CI* demonstrates an initial increase and subsequent decrease as the S_{max}/P ratio increases. Maximizing rock-breaking efficiency and minimizing cutter consumption are crucial for improving tunneling performance. In saturated conditions, the corresponding optimal S_{max}/P ratio ranges are 7.055–8.319 for soft rock, 8.606–8.931 for medium–hard rock, and 13.50–14.00 for hard rock, and these optimal ranges under dry conditions are 8.495–9.457, 10.972–12.169, and 16.5–17.5 for the same rock types. This study provides optimal S_{max}/P ratio ranges for TBM tunneling, thereby significantly enhancing tunneling efficiency.

Keywords: *CI*; water saturation effect; optimal tunneling parameters; disc cutter consumption

Citation: Wang, W.; Yan, C.; Guo, J.; Zhao, H.; Li, G.; Yao, W.; Ren, T. Improving Tunnel Boring Machine Tunneling Performance by Investigating the Particle Size Distribution of Rock Chips and Cutter Consumption. *Buildings* **2024**, *14*, 1124. https://doi.org/10.3390/buildings14041124

Academic Editor: Humberto Varum

Received: 5 March 2024
Revised: 12 April 2024
Accepted: 14 April 2024
Published: 17 April 2024

1. Introduction

Tunnel boring machines (TBMs) are extensively used in engineering projects, such as water conveyance tunnels, highway tunnels, and railway tunnels, owing to their exceptional rock-breaking efficiency, capacity for the provision of a secure working environment, and minimal impact on their geological surroundings. In the 21st century, China has achieved

remarkable advancements in the construction of extensive and large-scale tunnel projects through the utilization of the TBM method. Notable completed projects include the West Qinling Tunnel of the Lanzhou–Chongqing Railway, the Qinling Tunnel of the Xikang Railway, the Dahuofang Water Diversion Tunnel in Liaoning, the Shaanxi Water Diversion Tunnel from the Han to Wei Rivers, and the Jilin Water Diversion Project. The TBM method stands as one of the prevailing construction techniques for the creation of lengthy tunnels, with its primary advantage rooted in its rapid construction pace [1–4]. Consequently, while prioritizing the secure execution of TBM operations, paramount strategies encompass diminishing disc cutter consumption while enhancing rock-breaking efficiency.

During the TBM construction process, the mechanism of breaking rocks using the disc cutter is highly complex. A TBM employs a disc cutter for rotation and cutting, thereby inducing tensile, compressive, and shear failures within a rock mass as an integral part of the excavation process [5]. In the process of rock-breaking using a disc cutter, the efficiency of TBM rock-breaking is primarily influenced by several factors, including the properties of the surrounding rock, the TBM cutter head, and the tunneling parameters. On one hand, the presence of joints with varying orientations, inclinations, and integrity levels in the surrounding rock introduces complexity and uncertainty to the TBM rock-breaking mechanism. On the other hand, the arrangement of the disc cutters and the tunneling parameters of the TBM, including the spacing between TBM disc cutters and penetration, also exert substantial influences on the efficiency of rock-breaking. The spacing between TBM disc cutters can significantly impact the efficiency of rock-breaking. It is essential to note that the cutter head and cutters of a TBM cannot be altered or modified during the later stages of manufacturing and installation. Therefore, it is necessary to establish spacing reasonably based on the rock-breaking mechanism before manufacturing to optimize rock-breaking. Cho et al. [6] assessed the linear cutting performance of full-scale TBM disc cutters on granite under various conditions and identified an optimal cutter spacing range that enhanced the cutting performance of the disc cutters. Penetration refers to the depth to which the TBM disc cutter is pressed into the rock under the thrust of the cutter head, and the extent of penetration significantly influences the cutting effectiveness of a TBM disc cutter. Pan et al. [7] conducted full-scale linear cutting experiments on granite and sandstone under varying confining pressures. They observed that the specific energy (*SE*) exhibited a trend of initially decreasing and then increasing with an increase in penetration depth. There exists an optimal penetration depth that maximizes the cutting performance of the disc cutter. Gertsch et al. [8] investigated the impact of disc cutter spacing and penetration on the rock-breaking cutting performance of disc cutters through a series of rock-breaking experiments. They observed that *SE* is more responsive to variations in disc cutter spacing than penetration. The characteristics of the surrounding rock, the cutter spacing, and the penetration exert a substantial influence on the size and shape of the rock chips [9–11], particularly their impact on the rock-breaking efficiency of the TBM. Compared to the properties of the surrounding rock, cutter spacing and penetration are controllable. Therefore, in the TBM construction process, determining the optimal ratio of cutter spacing to penetration is of great significance for improving the rock-breaking efficiency of the TBM. Given the variation in cutter spacing at different positions and the fact that the maximum cutter spacing accounts for a large proportion of the cutter head, this study adopts the maximum cutter spacing as the TBM cutter spacing value. Numerous researchers have identified the optimal ratio of cutter spacing to penetration (*S/P*) through indoor linear cutting experiments [10]. These experiments entailed calculating *SE* using construction data measured at various *S/P* values, followed by the creation of a graphical representation illustrating the relationship between *SE* and the *S/P* ratio. The optimal ratio is determined by identifying the *S/P* value corresponding to the minimum *SE* on the graph. However, it is important to highlight that most indoor linear cutting experiments employ relatively small rock samples, which can restrict their ability to accurately represent real construction site conditions [12]. The studies mentioned above mainly rely on indoor

experiments, with minimal discussion and research devoted to assessing the effectiveness of TBM excavation based on insights gained from on-site construction data.

The tunneling performance of a TBM and the lifespan of its disc cutter are mainly influenced by factors including the characteristics of the surrounding rock, the TBM's design, the interaction between the cutter and the surrounding rock, and the engineering geological environment [13,14]. Additionally, the presence of water in the surrounding rock significantly affects TBM tunneling performance as it can cause changes in the dry and saturated conditions of the surrounding rock. This is due to variations in the mechanical properties of rock under dry and saturated conditions [15]. Currently, there is limited research on evaluating TBM rock-breaking efficiency and optimizing tunneling parameters under varying dry and saturated conditions in surrounding rock. For example, Mammen et al. [16] studied the impact of water on the cutting performance of enhanced linear tunneling machines. They observed that disc cutter consumption in saturated argillaceous quartz sandstone is approximately 20% less than in dry argillaceous quartz sandstone. Similarly, Bakar et al. [17] concluded that water saturation can reduce the thermal fatigue of cutters based on experiments involving cutting rocks with full-scale cutters. Mosleh et al. [18] observed that disc cutter consumption initially increases and then decreases as the water content in orthoquartz sandstone rises. Bakar et al. [19] conducted full-scale cutting experiments on dry and saturated test blocks of medium-strength sandstone using a linear rock-cutting machine. They found that the *SE* was relatively low during the process cutting of saturated sandstone, resulting in improved rock-breaking efficiency and speed. Zhu et al. [20] discovered that the minimum *SE* of saturated sandstone is about 17% greater than that of corresponding dry rocks. Although some scholars have examined the influence of water on the physical and mechanical properties of surrounding rock, there has been relatively limited research conducted on the effects of varying dry and saturated tunneling conditions on the rock-breaking efficiency and disc cutter consumption of TBMs. Therefore, it is crucial to investigate the impact mechanisms of various construction and environmental conditions on TBM operations. This will aid in selecting optimal tunneling parameters, ultimately reducing project timelines and minimizing construction costs.

Most of the aforementioned studies primarily ascertained the *S/P* value through indoor linear cutting experiments, which may not precisely reflect the actual situation of a construction site. However, there is a scarcity of research focused on optimizing TBM tunneling efficiency using construction site data, especially regarding the impact of varying dry and saturated conditions on TBM rock-breaking efficiency and disc cutter consumption. In recent years, artificial intelligence and machine learning have introduced new approaches for predicting TBM tunneling efficiency [21] and analyzing shield tunnel settlement [22]. However, a large amount of on-site data is required for training machine learning-based models. Consequently, a straightforward method based on statistics and a fitting analysis is employed in this study. Selecting the appropriate S_{max}/P ratio based on on-site construction data and considering various dry and saturated conditions in the surrounding rock is crucial. This decision guides TBM construction, enhances rock-breaking efficiency, and effectively reduces cutter consumption and construction costs.

Building on this foundation, this study derives *CI*, *SE*, and S_{max}/P ratio values from on-site sieving tests and construction logs, and the complex correlations among these variables are studied through data fitting. Additionally, this study investigates the impact of varying dry and saturated conditions on TBM tunneling efficiency by analyzing the data correlations between *CI* and the S_{max}/P ratio, as well as cutter consumption and the S_{max}/P ratio. The aim is to optimize TBM tunneling parameters at the construction site and provide valuable insights and practical guidance for engineering practices.

2. Project Background

The rock samples utilized in this study were collected from a water conveyance tunnel project that transports water from the Liujiaxia Reservoir to Lanzhou City in northwestern China (see Figure 1). This project encompasses water tunnels, branch lines, treatment

facilities, and municipal pipelines. The primary water conveyance tunnel was constructed using two double-shield TBMs that initiated tunneling from opposite ends. TBM 1 initiated tunneling from the Liujiaxia Reservoir side, while TBM 2 began from the Lujiaping water treatment plant side. These tunnel sections were designated TBM 1 and TBM 2, with lengths of 12.227 km and 13.259 km, respectively. The longitudinal gradient of the main tunnel averages approximately 0.1%. Initially, the main tunnel was designed with a diameter of 5.46 m, but it was measured at 4.60 m after construction. The maximum burial depth of the main tunnel reaches 918 m.

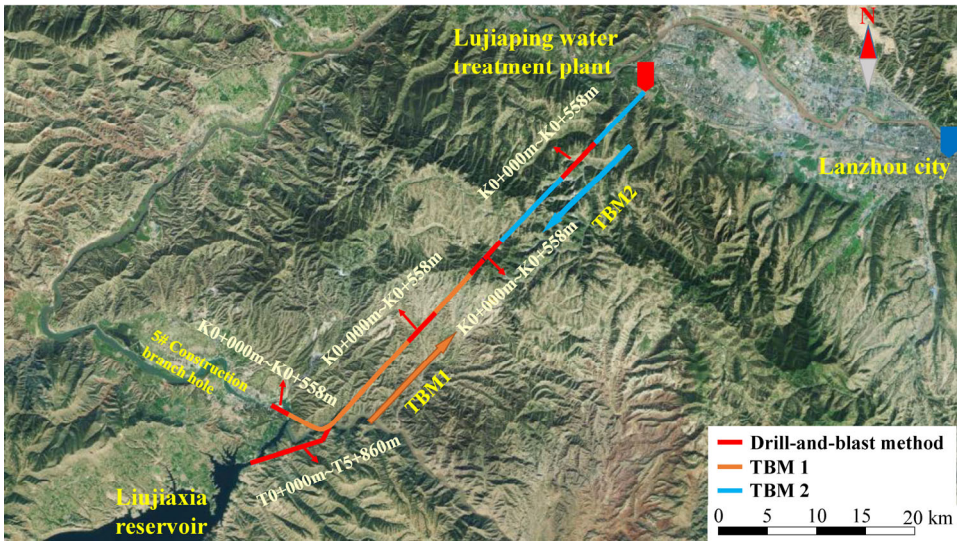

Figure 1. Construction layout of the water conveyance tunnel.

The geological profile along the water conveyance tunnel is shown in Figure 2. The lithology of the strata encountered along the water conveyance tunnel includes the following: (1) Middle Caledonian quartz diorite (δo_3^2); (2) blue-grey quartz schist of the pre-Sinian Mazhuanshan Group ($AnZmx^4$); (3) middle Caledonian granite (γ_3^2); (4) the Lower Cretaceous Hekou Group (K_1hk^1), characterized by brown-red interbedded with light gray-green sandstone and mudstone; and (5) green-gray metamorphic andesite of the Upper Middle Ordovician Wusu Mountain Group ($O_{2-3}wx^2$). The primary design parameters for TBM1 and TBM2 are provided in Table 1.

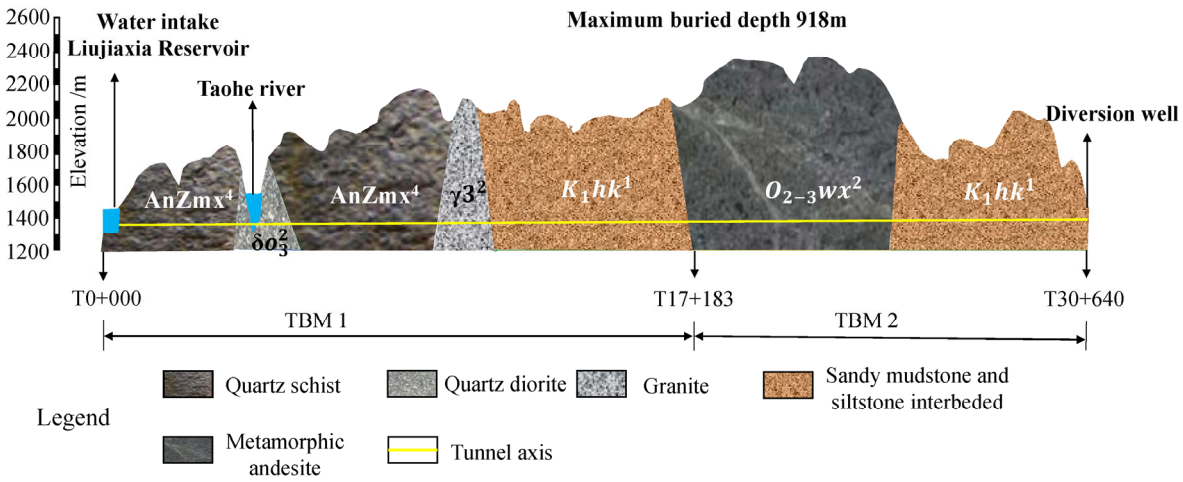

Figure 2. Geological profile of the water conveyance tunnel.

Table 1. TBM main design parameters.

TBM Design Parameters	Water Conveyance Tunnel	
	TBM1	TBM2
TBM type	double shield	
Tunneling diameter	5460 mm	5460 mm
Number of disc cutters	37	30
Center disc cutter/diameter	6/432 mm	4/432 mm
Inner cutter/diameter	21/483 mm	17/483 mm
Gauge cuter/diameter	10/483 mm	9/483 mm
Maximum cutter spacing	86 mm	83 mm
Cutter head speed	0~10.3 r·min^{-1}	0~8.7 r·min^{-1}
Cutter head power	1800 kW	2100 kW
Maximum cutter head thrust	22,160 kN	11,900 kN
Rating torque	3458 kN·m	4210 kN·m
Breakaway torque	5878 kN·m	6940 kN·m
Maximum tunneling speed	120 mm·min^{-1}	120 mm·min^{-1}

3. Rock Chip Sieving and Laboratory Tests

3.1. On-Site Rock Chip Sieving Test

Research has indicated that analyzing rock chip data generated during TBM tunneling is the primary method for evaluating a TBM's rock-breaking efficiency [23,24]. Rock chip sieving tests serve as a primary means of acquiring these crucial rock chip data. According to relevant European regulations (BSEN933-1-2012) [25], the minimum required sample weight for each sieve group depends on the maximum particle size of the rock chip, with a minimum of 40 kg mandated for samples with a maximum particle size of 63 mm. Therefore, to ensure the representativeness of collected rock chip samples, it is advisable to aim for a minimum mass of at least 100 kg for each group of samples.

The rock chip sieving test utilized standard square-hole sieves with apertures of 40 mm, 31.5 mm, 25 mm, 16 mm, 10 mm, 5 mm, and 2.5 mm to randomly select mixed particle-size rock chip samples from the TBM belt conveyor outlet at the construction site (see Figure 3). Subsequently, the fundamental data acquired from the TBM rock chips were employed for the analysis and assessment of the TBM's rock-breaking efficiency. Sampling should adhere to minimum sampling requirements such that each group of rock chips is manually or mechanically sieved, and the weights of rock chips with varying particle sizes, as obtained through sieving, are recorded. Dry rock chips can be directly sieved, while wet rock chips require natural drying before sieving.

Figure 3. The sieving test of TBM rock chips.

3.2. Preparation of Rock Samples

Following testing requirements and engineering geological survey data, representative rock cores from five distinct lithologies were extracted from the core library in the Lanzhou Water Conveyance Tunnel Project. During the sampling process, elongated and intact cylindrical rock cores were obtained from various depths of the geological drilling column, corresponding to metamorphic andesite (A), sandstone (S), granite (H), quartz schist (Y), and quartz diorite (SY). For each lithology, 6–8 rock core samples, each with a length of no less than 30 cm, were collected. Subsequently, following laboratory testing standards, these rock core samples were processed through various methods to prepare them for the Cerchar abrasion test. The original rock core test sections, representing the five distinct lithologies, were made into standardized cylindrical samples with a diameter of 50 ± 1 mm and a height of 40 ± 1 mm, following three steps: drilling, cutting, and grinding. The upper and lower surfaces of these samples were maintained parallel. There were 8 samples for each group, totaling 40 samples, each classified and assigned a unique identification number.

3.3. Cerchar Abrasivity Test

In this study, a rock abrasion servo tester (as depicted in Figure 4) was utilized to determine the Cerchar Abrasivity Index (*CAI*) values of 40 rock samples obtained from five distinct lithologies. The objective was to evaluate the wear resistance of the rocks. The instrument provides numerous advantages, including high levels of automation, compatibility with various test material shapes, user-friendly operation, and precise measurement capabilities.

To evaluate the impact of varying lithological rock *CAI* values on disc cutter consumption under both dry and saturated conditions, Cerchar abrasivity tests were conducted on rock samples exposed to these conditions (see Figure 5). The test procedure for this test followed the ASTM D7625-2010 [26] specification. A total of five groups of standard rock samples were prepared for the test, with each group containing eight samples. In each group, the first four rock samples (1–4) underwent Cerchar abrasion tests under dry conditions, whereas the subsequent four rock samples (5–8) underwent Cerchar abrasion tests under saturated conditions. The test results are presented in Table 2.

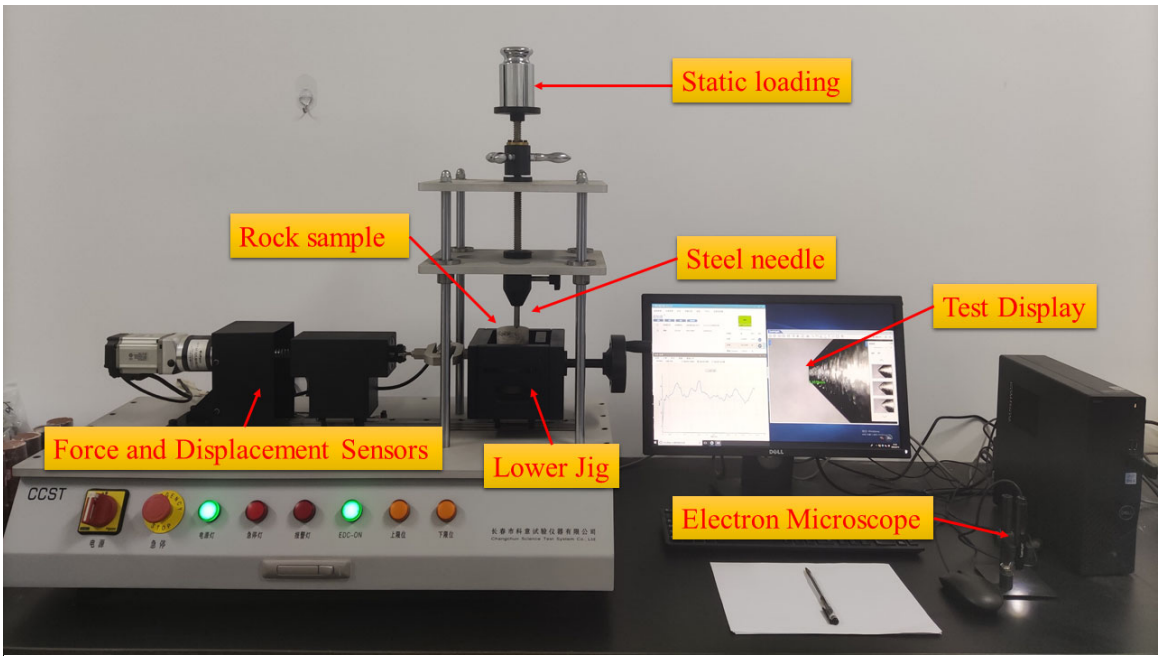

Figure 4. Rock abrasion servo tester.

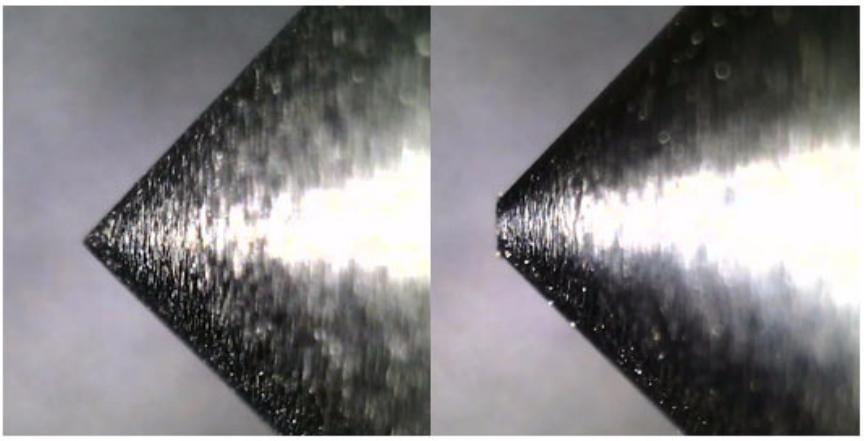

Figure 5. Steel needle evaluation before and after the Cerchar abrasion test.

Table 2. *CAI* values for rocks of different lithologies in dry and saturated conditions.

Rock Lithology	Code Name	Sample Number	CAI_{dry}	Average CAI_{dry}	Code Name	CAI_{sat}	Average CAI_{sat}
Metamorphic andesite	A	A1	2.435	2.530	A5	1.846	2.006
		A2	2.358		A6	1.553	
		A3	2.746		A7	2.439	
		A4	2.581		A8	2.184	
Sandstone	S	S1	0.751	0.846	SH5	0.564	0.747
		S2	0.978		SH6	0.939	
		S3	0.835		SH7	0.741	
		S4	0.821		SH8	0.743	
Granite	H	H1	2.933	3.523	H5	2.581	2.905
		H2	3.751		H6	2.943	
		H3	3.323		H7	3.261	
		H4	4.085		H8	2.834	
Quartz schist	Y	Y1	4.169	3.488	SP5	3.041	3.024
		Y2	3.323		SP6	2.822	
		Y3	3.647		SP7	3.254	
		Y4	2.813		SP8	2.978	
Quartz diorite	SY	SY1	3.539	3.167	SY5	3.219	3.102
		SY2	2.959		SY6	3.411	
		SY3	2.953		SY7	3.042	
		SY4	3.215		SY8	2.734	

4. Correlations among *CI*, *SE*, and Tunneling Parameters

The arrangement of a TBM's cutters plays a crucial role in determining its rock-breaking efficiency. Specifically, the ratio of maximum disc cutter spacing to penetration (S_{max}/P) significantly affects the characteristics of rock chip particle size and shape. Identifying the optimal value of the S_{max}/P ratio is essential for mitigating tunneling energy consumption, enhancing TBM rock-breaking efficiency, and reducing engineering costs. In engineering, the *CI* is widely embraced by researchers for its intuitive and convenient assessment of rock chip particle size distribution. Additionally, its simple calculation allows for an indirect evaluation of TBM rock-breaking efficiency. Therefore, employing the *CI* to determine the optimal S_{max}/P is not only straightforward and convenient but also offers more precise insight into on-site construction conditions. To provide a valuable reference for selecting tunneling parameters in similar projects, this section investigates the correlations among the *CI*, *SE*, and S_{max}/P ratio.

4.1. Specific Energy (SE)

SE is an indicator used to represent the amount of energy required to break a unit of rock mass. In recent years, with the widespread application of TBMs in tunnel construction, *SE* has become a common metric for evaluating the rock-breaking efficiency of TBMs in tunnel construction projects [27]. Usually, the smaller the *SE*, the less energy is required to cut a unit of rock mass, leading to a higher rock-breaking efficiency for the TBM and vice versa. The formula for calculating specific energy is as follows:

$$SE = \frac{F_v l + M\theta}{l\pi R^2} \quad (1)$$

where *SE* is the specific energy (kJ/m^3), F_v is the average tunneling thrust of the TBM (kN), l is the tunneling distance of the TBM for a certain period (m), M is the average torque of TBM tunneling (KN·m), θ is the rotation angle of the cutter (rad), and R is the radius of the excavated tunnel (m).

Through the extraction, analysis, and processing of data from construction logs related to various rock chips and tunneling parameters in the Lanzhou Water Conveyance Tunnel Project, *SE* was computed for each tunneling section, as shown in Tables 3 and 4.

Table 3. Sieving test data for rock chips cut by TBM for soft rocks and hard rocks.

Group Number	Surrounding Rock Grade	Sieve Quality (kg)	S_{max}/P	*SE* (kJ/m^3)	*CI*
1	IV	178.81	6.38	30,024.92	312.13
2	IV	108.20	5.2	31,784.36	279.29
3	III	215.17	9.8	19,939.43	347.60
4	III	164.30	5.4	29,866.75	326.74
5	III	119.80	9.5	17,356.68	366.00
6	III	104.61	7.22	27,396.53	328.00
7	III	194.37	9	19,616.44	350.66

Table 4. The sieving test data of rock chips cut by TBM for hard rocks.

Group Number	Surrounding Rock Grade	Sieve Quality (kg)	S_{max}/P	*SE* (kJ/m^3)	*CI*
1	II	180.50	22.25	78,505.88	377.28
2	II	171.15	23.25	68,820.04	350.74
3	II	263.17	20.11	51,575.24	430.81
4	II	212.74	12.29	32,221.89	448.88
5	II	175.07	12.6	29,259.62	454.06
6	II	239.25	17.2	38,060.04	457.58
7	II	214.14	20.5	46,150.56	429.67

4.2. Coarseness Index (CI)

Roxborough et al. [28] proposed the concept of the *CI*, which can, to a certain extent, reflect both the fragmentation of rock chips [24] and the distribution of particle sizes within the rock chips [29]. Utilizing data from the rock chip sieving tests, the particle size distribution of the rock chips is analyzed to calculate the cumulative residual rate for each sieve. Subsequently, these cumulative residual rates are aggregated to calculate the *CI*. The specific calculation expression is as follows:

$$X_i = \frac{W_i}{W_t} \times 100\% \quad (2)$$

$$CI = \sum X_i \quad (3)$$

where W_i is the total mass of rock chips larger than a certain particle size obtained from on-site sieving tests (kg); W_t is the total mass of TBM rock chips taken on-site (kg); X_i is

the cumulative residue rate greater than a certain particle size; *CI* is coarseness index of rock chips.

A total of 14 on-site rock chip sieving tests were completed, involving five typical rock types. Rock hardness varies and is categorized into two types of surrounding rock: hard rock and relatively soft rock, both of which are well representative. After sieving, we obtained data from 14 groups of TBM rock chip sieving tests, and the results of the sieving tests are presented in Tables 3 and 4. Through the analysis and processing of data obtained from on-site rock chip sieving tests, *CI* indicators can be derived for both soft rock and hard rock. Construction data were collected, and *SE* values for the two working conditions were calculated using Equation (1), as presented in Tables 3 and 4.

4.3. Correlation between CI and SE

The rock mass information at the construction site was divided into two working conditions: soft rock and hard rock. A correlation analysis of the *CI* and *SE* for these two working conditions is presented in Figure 6.

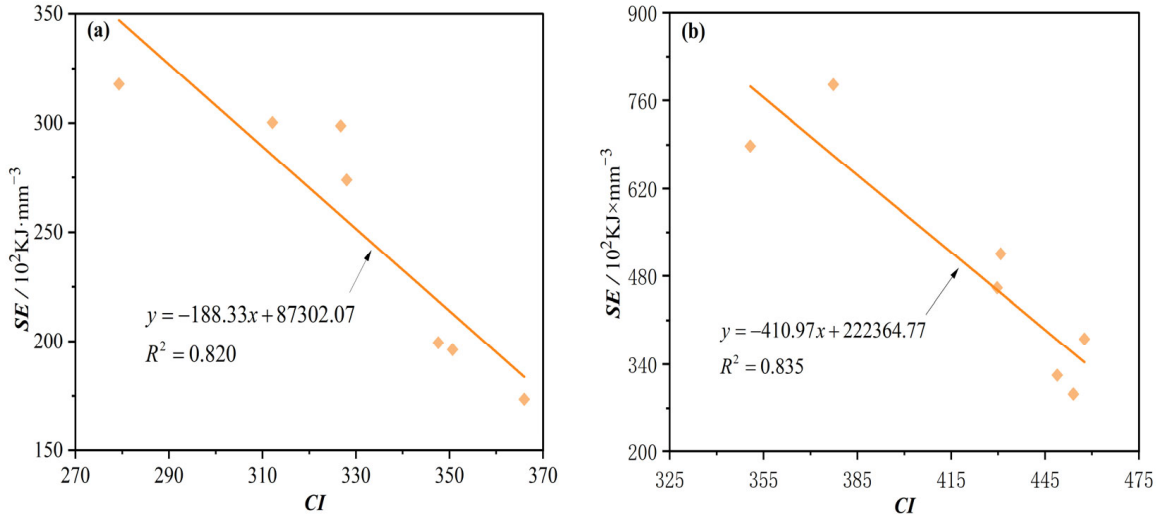

Figure 6. Correlation between *CI* and *SE*. (**a**) Soft rocks; (**b**) hard rocks.

As shown in Figure 6, in both soft rock and hard rock conditions, *SE* decreases as the *CI* increases. The correlation between these two parameters is strong, with correlation coefficients of 0.820 and 0.835, respectively. This indicates that the *CI* maintains a robust linear correlation with *SE*, offering an accurate reflection of the TBM's rock-breaking efficiency. From the perspective of the rock chip analysis, when the TBM exhibits high rock-breaking efficiency, the proportion of block and sheet rock chips is relatively high, whereas the content of powdered rock chips is comparatively low, resulting in a higher calculated *CI*. Conversely, when the TBM's rock-breaking efficiency is low, there are lower contents of block and sheet rock chips, while the content of powdered rock chips is higher, resulting in a lower calculated *CI*. Thus, using the *CI* to reflect the rock-breaking efficiency of a TBM is reliable. Furthermore, the considerable variability in parameters like thrust, torque, and penetration at TBM construction sites often poses challenges in accurately determining the parameter values required for calculating *SE*. In some cases, it becomes extremely challenging to accurately calculate *SE* for a construction site. Obtaining corresponding *CI* indicators from the rock chips generated in real time during TBM tunneling can be achieved through a relatively straightforward method, offering precise feedback on on-site construction conditions. Therefore, the optimization of TBM tunneling parameters and the provision of feedback on rock-breaking efficiency based on the *CI* hold significant practical significance.

4.4. Correlation between Rock-Breaking Efficiency and Tunneling Parameters

Data from 14 on-site rock chip sieving tests and the calculated *CI*, *SE*, and S_{max}/P values from TBM construction logs (Tables 3 and 4) were utilized to examine and analyze the correlation between S_{max}/P and *SE*, as well as between S_{max}/P and *CI*. The results are presented in Figures 7 and 8.

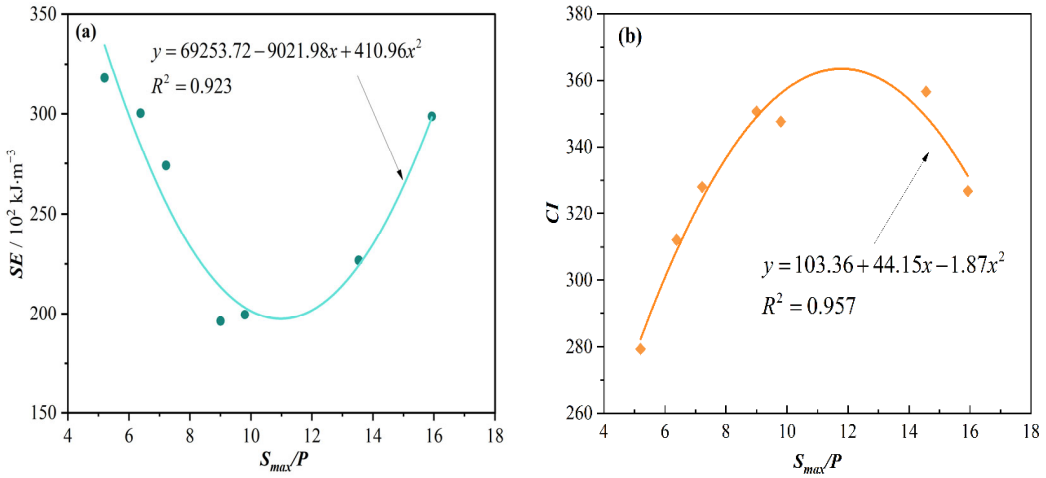

Figure 7. Correlations between *SE* and S_{max}/P ratio and *CI* and S_{max}/P ratio for soft rock. (**a**) Correlation between S_{max}/P ratio and *SE*; (**b**) correlation between S_{max}/P ratio and *CI*.

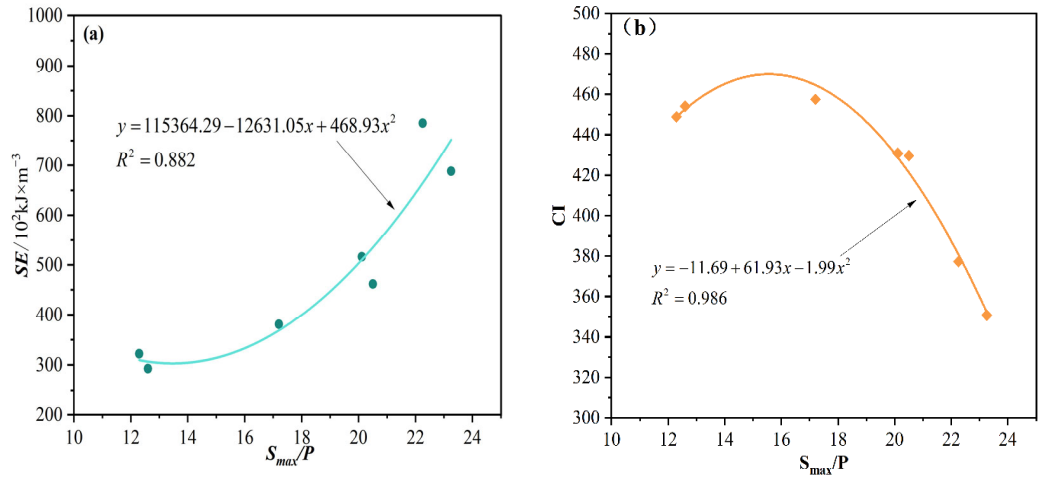

Figure 8. Correlations between *SE* and S_{max}/P ratio as well as *CI* and S_{max}/P ratio for hard rock. (**a**) Correlation between S_{max}/P ratio and *SE*; (**b**) correlation between S_{max}/P ratio and *CI*.

From Figures 7 and 8, it is evident that under all operating conditions, the *SE* initially decreases and subsequently increases with an increase in the S_{max}/P ratio. An optimal S_{max}/P value exists to minimize *SE*. Similarly, the *CI* initially increases and then decreases with the increase in the S_{max}/P ratio, and an optimal S_{max}/P value can be identified to maximize the *CI*. When the S_{max}/P ratio is small (indicating higher penetration), thrust and torque on the cutter head increase, strengthening the synergistic effect among the TBM's cutters. This leads to excessive rock-breaking, as depicted in Figure 9a, in which predominantly block-shaped rock chips prevail. The energy provided by the TBM is greater than the energy required for rock-breaking, resulting in an increase in the ineffective rock-breaking energy and a relatively lower rock-breaking efficiency. As the S_{max}/P ratio increases, particularly within the optimal S_{max}/P range, the penetration becomes moderate, allowing cracks initiated by neighboring disc cutters to gradually extend to the penetration point, effectively breaking the rock. This is illustrated in Figure 9b, in which the predominant form of rock

chips is in the shape of flakes. At this stage, energy consumption is minimized, resulting in effective rock-breaking. However, with a continued S_{max}/P increase, the penetration is relatively low, and the synergy between TBM cutters weakens. The cracks generated by disc cutters cannot link up to each other. The primary reason for this phenomenon is that under conditions of reduced driving force, the cutting force applied by the disc cutter fails to reach the critical load required for rock-breaking [30]. Consequently, a grinding effect occurs between the disc cutter and the rock, resulting in increased powdery rock chip content, smaller rock chip particle sizes, an elevated *SE*, and a reduced *CI*. Therefore, the rock-breaking efficiency of the TBM decreases [31], as illustrated in Figure 9c. During this period, penetration is minimal, resulting in limited rock-breaking and slower tunneling progress, which is not conducive to efficient tunneling.

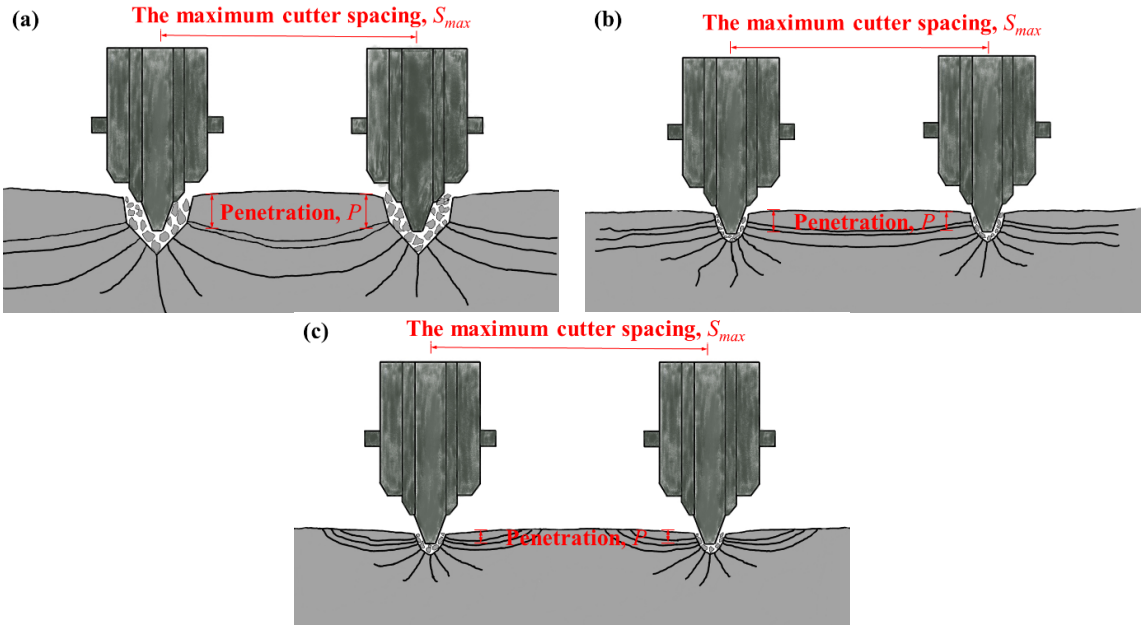

Figure 9. Disc cutter rock-breaking methods at different S_{max}/P values. (**a**) Smaller S_{max}/P value, (**b**) optimal S_{max}/P value, and (**c**) greater S_{max}/P value.

Additionally, as shown in Figures 7 and 8, both *SE* and the *CI* exhibit a strong quadratic correlation with S_{max}/P values under both operational conditions, with fitting coefficients exceeding 0.880. Specifically, Figure 7 indicates a quadratic fitting coefficient between *SE* and the S_{max}/P ratio of 0.923, with the optimal S_{max}/P range identified as 10–12 under soft rock conditions. Similarly, the quadratic fitting coefficient between the *CI* and S_{max}/P ratio is 0.957, with the optimal S_{max}/P range being 11–12. In Figure 8, the quadratic fitting coefficient between *SE* and the S_{max}/P ratio is 0.882, with an optimal S_{max}/P range of 13–14 under hard rock conditions. Similarly, the quadratic fitting coefficient between the *CI* and S_{max}/P ratio is 0.986, with the optimal S_{max}/P range determined to be 15–16. Under both working conditions, the *CI* exhibits superior quadratic fitting coefficients compared to the *SE*, with percentages of 4.2% and 10.6% higher, respectively. This suggests that the *CI* offers a more precise fit with respect to the S_{max}/P ratio. Moreover, the *CI* is more readily obtainable at the construction site and offers higher accuracy compared to *SE* indicators. Therefore, the *CI* possesses unparalleled advantages in the optimization of TBM tunneling parameters and in guiding on-site TBM construction.

5. Influence of Dry and Saturated Conditions on TBM Tunneling Efficiency and Optimization of Tunneling Parameters

In the majority of engineering projects employing TBM construction, the prevailing conditions for the surrounding rock typically fall into two categories: dry and saturated states. To explore the influence of the presence of water on the properties of different

tunnel-surrounding rocks and TBM tunneling efficiency, the Cerchar Abrasivity Test was conducted using data from the Lanzhou Water Conveyance Tunnel Project. Tunneling data from TBM sections with varying lithologies were collected, organized, and subjected to a fitting analysis. This study explores differences in TBM rock-breaking efficiency and cutter consumption under different dry and saturated tunneling conditions. Furthermore, TBM tunneling parameters were optimized based on the principle of maximizing the *CI* and minimizing disc cutter consumption. By identifying the optimal tunneling parameters for various tunneling conditions, the objective of enhancing TBM rock-breaking efficiency and minimizing TBM disc cutter consumption was accomplished.

5.1. Optimization of Tunneling Parameters Based on CI

At the TBM construction site of the Lanzhou Water Conveyance Tunnel Project, tunneling sections involving relatively soft rock (sandstone), medium-hard rock (metamorphic andesite), and hard rock (granite, quartz schist, and quartz diorite) were selected for collecting, statistically analyzing, and processing TBM tunneling data. Corresponding rock chip samples were also collected for sieving tests. A robust quadratic relationship exists between the S_{max}/P ratio and the *CI*, with the *CI* serving as a superior indicator for assessing TBM rock-breaking efficiency and on-site construction conditions. Therefore, sieving tests were conducted on the aforementioned types of rock chips. Based on the sieving results, the *CI* was calculated using Equations (2) and (3). The correlation between the *CI* and S_{max}/P ratio under various tunneling conditions was subjected to a fitting analysis, and the corresponding results are presented in Figure 10.

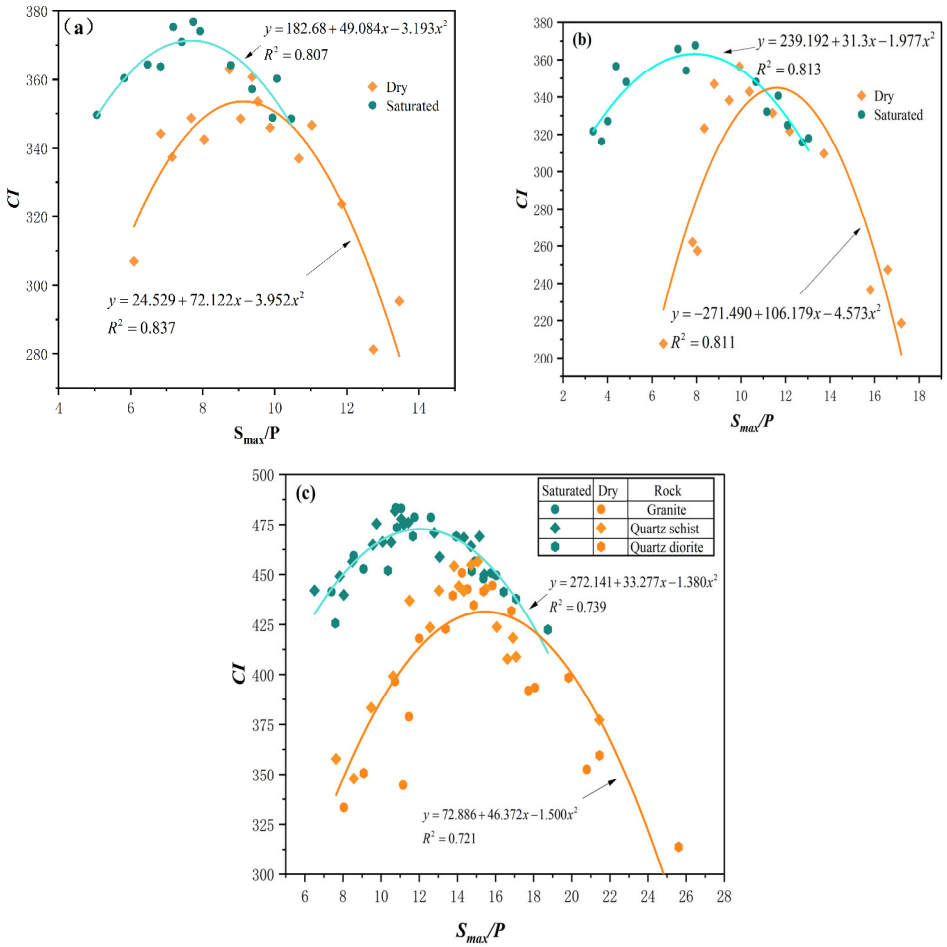

Figure 10. *CI* and S_{max}/P ratio relationship curves in dry and saturated conditions. (**a**) Relatively soft rock, (**b**) medium-hard rock, and (**c**) hard rock.

As shown in Figure 10, the correlation between the *CI* and the S_{max}/P ratio aligns with the previously analyzed results. A comparative analysis of Figure 10a–c reveals that for dry surrounding rocks classified as medium-hard rock (metamorphic andesite), relatively soft rock (sandstone), and hard rock (granite, quartz schist, and quartz diorite), the optimal S_{max}/P ranges for a TBM are 10.972–12.246, 8.495–9.749, and 14.511–16.640, respectively. Similarly, for saturated surrounding rocks classified as medium-hard rock (metamorphic andesite), relatively soft rock (sandstone), and hard rock (granite, quartz schist, and quartz diorite), the optimal S_{max}/P intervals for TBM are 7.187~8.641, 7.055~8.319, and 10.945~13.163, respectively. As observed in Figure 10, the curve representing saturated surrounding rock appears positioned higher and to the left compared to the curve representing dry surrounding rock. This is because of the lower strength of saturated surrounding rock. On one hand, the overall P tends to be higher due to saturation, while S_{max} remains unchanged. Consequently, the ratio S_{max}/P becomes smaller, leading to the curve of saturated surrounding rock being located to the left of that of dry surrounding rock. On the other hand, the lower strength of saturated surrounding rock contributes to a more effective rock-breaking efficiency, resulting in the relationship curve being positioned above that of dry surrounding rock. When the surrounding rocks consist of medium-hard rock (metamorphic andesite), relatively soft rock (sandstone), and hard rock (granite, quartz schist, and quartz diorite), the maximum *CI* of the TBM in the saturated state of the surrounding rock is, respectively, 5.27%, 5.01%, and 9.59% higher than that in the dry condition. This difference is attributed to the influence of water, which significantly weakens particle-to-particle bonding, reduces their binding force, and enhances the propensity for outward particle expansion [32]. The presence of water within the pores of the rock diminishes the strength and deformation characteristics of the rock, facilitating rock-breaking. Additionally, water exerts softening, dissolution, and water-wedge effects on rocks. When water molecules infiltrate the interstices among rock particles, they reduce the cohesion among these particles, leading to a decline in rock strength and a softening effect which is manifested by reductions in both strength and deformation parameters. Water, acting as a solvent, can dissolve certain mineral components within rock, leading to uneven stress or the partial dissolution of cementitious substances within the rock, thus playing a pivotal role in rock dissolution. Simultaneously, a reduction in pore volume during rock compression can induce an elevated pore water pressure, resulting in the generation of additional stress near the crack. This can trigger crack propagation and ultimately diminish the rock's yield and peak limit [33].

5.2. Optimization of Tunneling Parameters Based on Cutter Consumption

The data on TBM disc cutter consumption under five different rock tunneling conditions in the Lanzhou Water Conveyance Tunnel Project were collected and statistically analyzed, as presented in Table 5 and Figure 11. Figure 11 illustrates the varying impact of *CAI* values on TBM disc cutter consumption in rocks under different dry and saturated conditions. Regardless of whether the rock is dry or saturated, the consumption of TBM cutters increases exponentially with an increase in rock *CAI*. However, when the *CAI* is the same, the quantity of cutter consumption during TBM tunneling in saturated surrounding rock is observed to be lower than that in dry surrounding rock. Variations in TBM cutter consumption can be observed between dry and saturated conditions when tunneling surrounding rocks of differing *CAI* values. When the surrounding rock is sandstone with a lower *CAI*, the TBM cutter consumption of rocks in dry and saturated conditions is relatively low, and the difference is not significant. This is attributed to the fact that when the rock *CAI* is low, its hardness is relatively lower compared to the TBM disc cutter, and the influence of water within the rock's internal pores on softening the rock and its subsequent impact on TBM disc cutter consumption can be largely disregarded. However, in the case of metamorphic andesite, which is characterized by high wear resistance, TBM cutter consumption in saturated surrounding rock is reduced by 53.12% compared to dry surrounding rock. In scenarios involving granite, quartz schist, and quartz diorite, which possess the highest

wear resistance, TBM cutter consumption decreases by approximately 41.93% to 57.06% under saturated conditions relative to dry conditions. The consumption of TBM cutters under dry conditions of highly wear-resistant surrounding rock increases higher than that in the saturated condition as the *CAI* of the rock increases. This is attributed to the presence of water, which softens the rock, diminishes its strength, provides lubrication, and cools the rock. Additionally, it weakens the friction between the disc cutter and the rock surface, thereby reducing thermal fatigue wear induced by TBM disc cutter rock-breaking [34]. Water molecules infiltrate the internal pores of rocks, thereby diminishing the cohesion between mineral particles within the rock. Furthermore, as a solvent, water dissolves soluble mineral components, which further disrupts the internal structural cohesion of the rock, leading to a non-uniform stress distribution in terms of magnitude and direction within the rock. This is evidenced by a decrease in both the strength and deformation parameters of the rock [33]. Therefore, in the presence of rock with high wear resistance, the water within the rock's internal pores significantly influences the consumption of TBM cutters. Hence, gaining insight into the cutter consumption patterns of TBMs under varying lithologies and in both dry and saturated conditions can facilitate informed decisions for TBM disc cutter selection and design. It allows for the proposal of optimization measures tailored to geological conditions. Additionally, it enables the anticipation of disc cutter consumption during the construction process, leading to the prediction of cutter longevity and the optimization of cutter management strategies. This holds significant implications for enhancing TBM tunneling efficiency.

Table 5. *CAI* values and cutter consumption for dry and saturated rock.

Rock Lithology	Dry		Saturated	
	CAI_{dry}	Cutter Consumption 10^{-3} Piece m^{-3}	CAI_{sat}	Cutter Consumption (10^{-3} Piece·m^{-3})
Metamorphic andesite	2.530	2.568	2.006	1.204
Sandy stone	0.846	0.669	0.747	0.642
Granite	3.523	5.640	2.905	2.422
Quartz schist	3.488	6.070	3.024	2.741
Quartz diorite	3.167	5.066	3.102	2.942

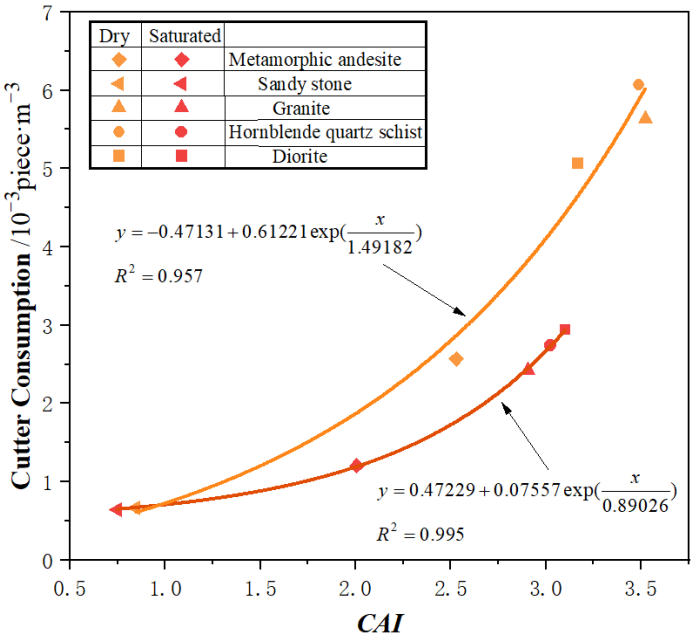

Figure 11. Cutter consumption variation with *CAI* in dry and saturated conditions.

The dry and saturated conditions, as well as the strength and wear resistance of the surrounding rock, significantly influence the consumption of TBM disc cutters. In practical engineering, the cost of cutters constitutes a significant portion of TBM construction projects, and the consumption of TBM disc cutters is notably influenced by tunneling parameters. There should be a connection between the S_{max}/P ratio and cutter consumption. Hence, it is imperative to investigate and analyze the correlation between TBM cutter consumption and the S_{max}/P ratio. By collecting, statistically analyzing, processing, and analyzing cutter consumption data during TBM construction, the corresponding tunneling data were selected to establish a correlation curve between TBM cutter consumption and the S_{max}/P ratio under varying dry and saturated conditions, as shown in Figure 11. As shown in Figure 11, regardless of whether the surrounding rock is classified as hard or soft rock and under both dry and saturated conditions, TBM cutter consumption initially decreases and subsequently increases with a rise in the S_{max}/P ratio. The optimal S_{max}/P ratio minimizes TBM cutter consumption by increasing the contact area between the disc cutter and the rock, thereby enhancing the synergistic effect among the TBM's disc cutters. The rock between the disc cutters exerts a counterforce on them, leading to friction between the disc cutter and the rock. When the S_{max}/P ratio is small, penetration is greater (with the cutter spacing remaining constant during tunneling), leading to increased friction between the cutter and the rock, thus resulting in greater TBM cutter wear. Within the optimal range of the S_{max}/P ratio, moderate penetration allows for the gradual extension of cracks generated by neighbor cutter heads, effectively facilitating rock-breaking. At this time, TBM tunneling efficiency is elevated, accompanied by a relatively modest consumption of TBM cutters. As the S_{max}/P ratio continues to rise, penetration decreases, leading to a diminished synergistic effect among TBM cutters. However, the total duration of contact friction between the cutters and the rock increases, leading to a relatively higher wear rate of TBM cutters. Therefore, the consumption of TBM cutters is higher, leading to decreased TBM tunneling efficiency during this period.

Comparing and analyzing Figure 12, optimal S_{max}/P ranges for TBMs are found to vary under different dry and saturated conditions with surrounding rock types. In the case of dry surrounding rocks, including medium-hard rock (metamorphic andesite), relatively soft rock (sandstone), and hard rock (granite, quartz schist, and quartz diorite), the optimal S_{max}/P ranges are 10.414~12.169, 7.976~9.457, and 17.465~19.369, respectively. Meanwhile, for saturated surrounding rocks of the same types, the optimal S_{max}/P ranges are 8.606~11.656, 6.502~8.769, and 14.514~16.193. The optimal S_{max}/P ratio for saturated surrounding rock is smaller than in dry conditions. The presence of water in the surrounding rock diminishes rock wear resistance and weakens the thermal fatigue wear of the disc cutter. Under identical penetration conditions, the wear resistance of saturated surrounding rock decreases, resulting in a relative reduction in TBM cutter consumption. Therefore, accurate predictions for cutter consumption under various dry and saturated conditions during tunneling can be made. Simultaneously, determining the optimal tunneling parameters under specific conditions also aids in reducing cutter consumption.

5.3. Optimal Tunneling Parameters Considering CI and Cutter Consumption

In TBM construction projects, the balance between rock-breaking efficiency and cutter consumption is frequently inadequate, potentially leading to project delays and increased costs. The construction period and cost are paramount concerns for enterprises involved in engineering projects. Therefore, it is imperative to comprehensively assess the rock-breaking efficiency and cutter consumption of a TBM, aiming to identify the optimal tunneling parameter range for maximizing its tunneling efficiency.

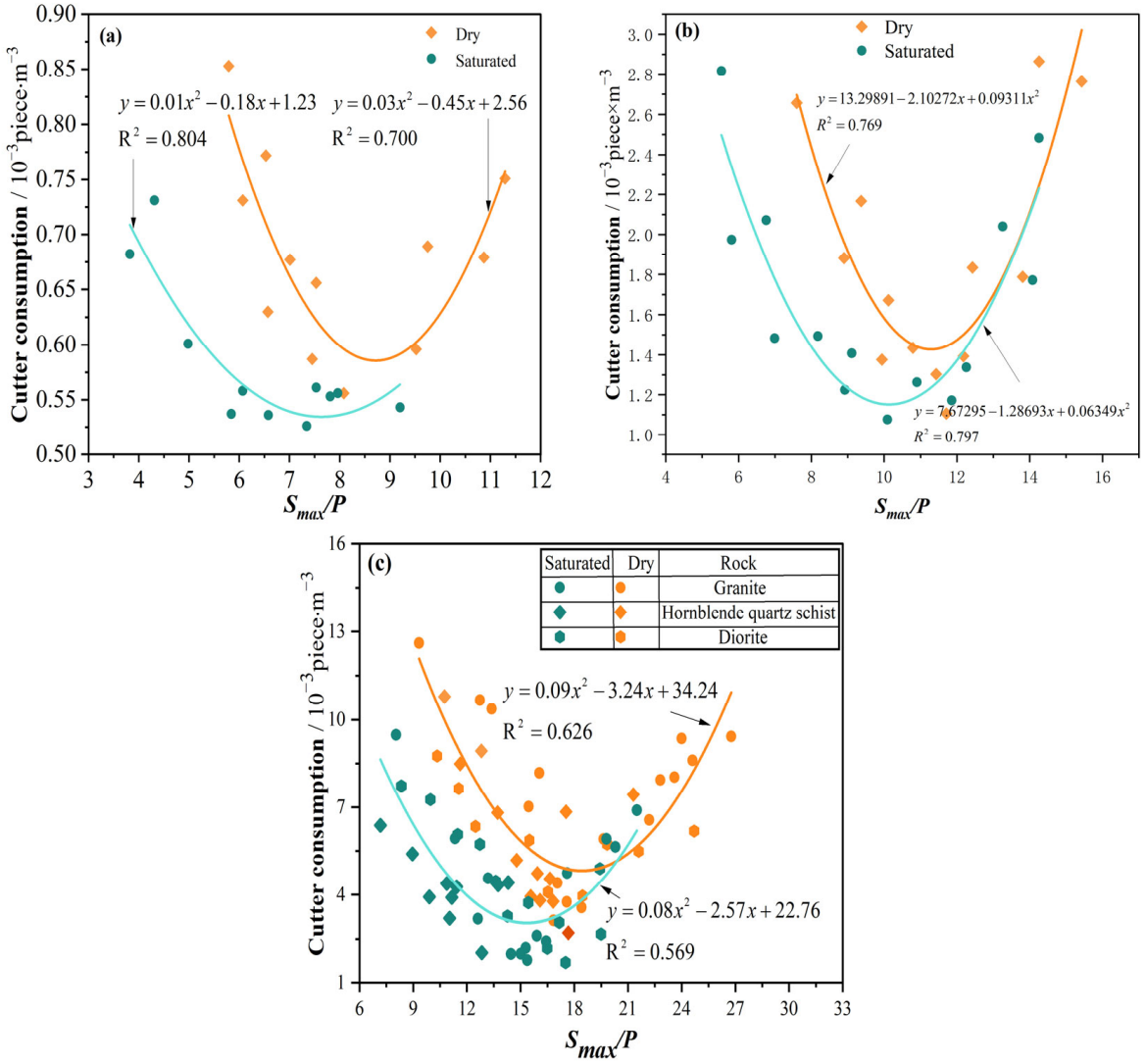

Figure 12. Cutter consumption variation with S_{max}/P ratio in dry and saturated conditions. (**a**) Relatively soft rock, (**b**) medium-hard rock, and (**c**) hard rock.

By comprehensively examining the correlations between the *CI* and the S_{max}/P ratio, as well as cutter consumption and the S_{max}/P ratio under varying dry and saturated conditions of the surrounding rock, this study analyzes TBM tunneling efficiency to optimize TBM tunneling parameters. Based on Figures 10 and 12, it is evident that for relatively soft surrounding rock, considering the *CI* and cutter consumption, the optimal S_{max}/P ranges for a TBM in dry and saturated conditions are 8.495~9.457 and 7.055~8.319, respectively. For medium-hard surrounding rock, considering the *CI* and cutter consumption, the optimal S_{max}/P ranges for TBMs in dry and saturated conditions are 10.972~12.169, and 8.606~8.931, respectively. At this time, TBMs exhibit enhanced rock-breaking efficiency with reduced cutter consumption. Considering the wide ranges of rock types analyzed in this study and the numerous factors influencing the properties of surrounding rocks, the optimal S_{max}/P range, based on the *CI* and cutter consumption, does not overlap for either dry or saturated conditions for hard rock. Recommended ranges were selected based on a data analysis and construction experience. The optimal S_{max}/P ranges for dry and saturated conditions are as follows: 16.5~17.5 and 13.50~14.00. The recommended optimal S_{max}/P ratio range is shown in Table 6. Figures 10 and 12 illustrate that within the optimal S_{max}/P range for TBM, rock-breaking efficiency is higher, while cutter consumption is minimized. Moreover, when the S_{max}/P value falls within the optimal range, the rock-breaking efficiency and

cutter consumption of a TBM in saturated rock conditions are more favorable for project advancement compared to dry conditions. The presence of water facilitates rock-breaking, reduces its wear resistance, and enhances the thermal fatigue wear of disc cutters. This study assessed the influence of varying dry and saturated conditions in the surrounding rock on TBM tunneling efficiency by employing data fitting while considering the *CI* and cutter consumption. The proposed optimal tunneling parameter range, considering both the *CI* and cutter consumption, can serve as a valuable reference for projects in similar geological conditions seeking to maximize TBM tunneling performance. This research holds significant implications for the optimization of TBM tunneling parameters, ultimately resulting in reduced project durations and construction costs.

Table 6. Optimal S_{max}/P ranges determined based on disc cutter consumption and *CI* data.

Rock Lithology		Soft Rock	Medium-Hard Rock	Hard Rock
The optimal S_{max}/P range determined based on *CI*	Dry	7.976~9.457	10.414~12.169	17.465~19.369
	Sat	6.502~8.769	8.606~11.656	14.514~16.193
The optimal S_{max}/P range determined based on cutter consumption	Dry	8.495–9.749	10.972–12.246	14.511–16.640
	Sat	7.055~8.319	7.187~8.641	10.945~13.163
The optimal S_{max}/P range recommendation	Dry	8.495~9.457	10.972~12.169	16.5~17.5
	Sat	7.055~8.319	8.606~8.931	13.50~14.00

6. Conclusions

A TBM parameter optimization method based on the *CI* and cutter consumption was proposed in this study based on the construction project of the water conveyance tunnel in the Lanzhou Water Conveyance Tunnel Project. This method effectively improves the rock-breaking efficiency of a TBM and reduces its cutting tool consumption. It employed a statistical analysis and data fitting to realize optimization. These findings provide valuable insights for the selection of tunneling parameters in similar engineering projects. The main research conclusions are as follows:

1. Both *SE* and the *CI* exhibit strong quadratic relationships with the S_{max}/P ratio. The fitting coefficients for the *CI* under both soft and hard rock conditions are 4.2% and 10.4% higher than those of the *SE*, respectively.
2. Regardless of if conditions are dry or saturated, TBM cutter consumption increases exponentially with the *CAI*. In different lithologies under saturated conditions, cutter consumption is 15.07% to 57.06% lower compared to dry conditions.
3. In both dry and saturated conditions, the *CI* initially increases and then decreases with an increase in the S_{max}/P ratio, while TBM cutter consumption decreases initially and then increases with a rise in the S_{max}/P ratio. There exists an optimal S_{max}/P value that maximizes TBM rock-breaking efficiency and minimizes TBM cutter consumption.
4. Considering both TBM rock-breaking efficiency and cutter consumption, the optimal S_{max}/P ranges for dry conditions are 10.972–12.169, 8.495–9.457, and 16.5–17.5 for medium-hard, soft, and hard rocks, respectively. In saturated conditions, the optimal S_{max}/P ranges are 8.606–8.931, 7.055–8.319, and 13.50–14.00 for the same rock types. To enhance TBM construction guidance, optimal tunneling parameter ranges are suggested for various dry and saturated surrounding rock tunneling conditions.

In conclusion, this optimization method can optimize the TBM parameters of similar geological formations by calculating the *CI* and cutter consumption. The efficiency optimization method proposed in this study is applicable to continuous strata, but its effectiveness for broken formations requires further investigation. However, the research methodology of this study is applicable to most strata and engineering projects. Subsequent research should collect more data for analysis and study a wider range of strata types. Further mechanical studies are warranted to facilitate TBM optimization design across diverse geological and environmental contexts.

Author Contributions: Conceptualization, W.W.; Project administration, W.W.; Supervision, W.W.; methodology, C.Y.; validation, W.Y. and T.R.; formal analysis, G.L. and J.G.; investigation, C.Y. and H.Z.; Resources, W.W. and T.R.; data curation, G.L. and H.Z.; writing—original draft preparation, J.G.; writing—review and editing, C.Y. and W.Y. All authors have read and agreed to the published version of the manuscript.

Funding: This work was supported by the National Natural Science Foundation of China (41972270), the Opening Foundation of the State Key Laboratory of Shield Machine and Boring Technology (SKLST-2019-K06), the Research Fund of the Key Laboratory of Water Management and Water Security for Yellow River Basin, Ministry of Water Resources (under construction) (2022-SYSJJ-06), the Science and Technology Program of China Railway 14th Bureau Group Co., Ltd. (91370000163055989120 21C03), and the Technology Project of State Grid Xinyuan Group (Holdings) Co., Ltd. (SGXYKJ-2022-050).

Data Availability Statement: The original contributions presented in this study are included in the article material; further inquiries can be directed to the corresponding author.

Conflicts of Interest: Wei Wang and Taozhe Ren were employed by the company State Grid Xinyuan Group (Holdings) Co., Ltd.; Gaoliu Li was employed by the company SGIDI Engineering Consulting (Group) Co., Ltd. The remaining authors declare that the research was conducted in the absence of any commercial or financial relationships that could be construed as a potential conflict of interest. The authors declare that this study received funding from the Science and Technology Program of China Railway 14th Bureau Group Co., Ltd. and the Technology Project of State Grid Xinyuan Group (Holdings) Co., Ltd. The funders had the following involvement with the study: Conceptualization, Wei Wang; validation, Wei Wang; formal analysis, Taozhe Ren; data curation, Taozhe Ren.

References

1. Liu, Q.S.; Huang, X.; Gong, Q.M.; Du, L.J.; Pan, Y.C.; Liu, J.P. Application and Development of Hard Rock TBM and Its Prospect in China. *Tunn. Undergr. Space Technol.* **2016**, *57*, 33–46. [CrossRef]
2. Huang, X.; Liu, Q.S.; Shi, K.; Pan, Y.C.; Liu, J.P. Application and Prospect of Hard Rock TBM for Deep Roadway Construction in Coal Mines. *Tunn. Undergr. Space Technol.* **2018**, *73*, 105–126. [CrossRef]
3. Armetti, G.; Migliazza, M.R.; Ferrari, F.; Berti, A.; Padovese, P. Geological and Mechanical Rock Mass Conditions for TBM Performance Prediction. The Case of "La Maddalena" Exploratory Tunnel, Chiomonte (Italy). *Tunn. Undergr. Space Technol.* **2018**, *77*, 115–126. [CrossRef]
4. Feng, S.X.; Chen, Z.Y.; Luo, H.; Wang, S.Y.; Zhao, Y.F.; Liu, L.P.; Ling, D.S.; Jing, L.J. Tunnel Boring Machines (TBM) Performance Prediction: A Case Study Using Big Data and Deep Learning. *Tunn. Undergr. Space Technol.* **2021**, *110*, 103636. [CrossRef]
5. Mao, H.M.; Chen, K.; Feng, H.H. Rock-breaking mechanism of TBM with different types of cutter tools and estimation of thrust force. *Chin. J. Geotech. Eng.* **2013**, *35*, 1627–1633. (In Chinese)
6. Cho, J.W.; Jeon, S.; Jeong, H.Y.; Chang, S.H. Evaluation of Cutting Efficiency during TBM Disc Cutter Excavation within a Korean Granitic Rock Using Linear-Cutting-Machine Testing and Photogrammetric Measurement. *Tunn. Undergr. Space Technol.* **2013**, *35*, 37–54. [CrossRef]
7. Pan, Y.C.; Liu, Q.S.; Liu, J.P.; Liu, Q.; Kong, X.X. Full-Scale Linear Cutting Tests in Chongqing Sandstone to Study the Influence of Confining Stress on Rock Cutting Efficiency by TBM Disc Cutter. *Tunn. Undergr. Space Technol.* **2018**, *80*, 197–210. [CrossRef]
8. Gertsch, R.; Gertsch, L.; Rostami, J. Disc Cutting Tests in Colorado Red Granite: Implications for TBM Performance Prediction. *Int. J. Rock Mech. Min. Sci.* **2007**, *44*, 238–246. [CrossRef]
9. Farrokh, E.; Rostami, J. Correlation of Tunnel Convergence with TBM Operational Parameters and Chip Size in the Ghomroud Tunnel, Iran. *Tunn. Undergr. Space Technol.* **2008**, *23*, 700–710. [CrossRef]
10. Han, D.Y.; Cao, P.; Liu, J.; Zhu, J.B. An Experimental Study of Dependence of Optimum TBM Cutter Spacing on Pre-Set Penetration Depth in Sandstone Fragmentation. *Rock Mech. Rock Eng.* **2017**, *50*, 3209–3221. [CrossRef]
11. Moon, T.; Oh, J. A Study of Optimal Rock-Cutting Conditions for Hard Rock TBM Using the Discrete Element Method. *Rock Mech. Rock Eng.* **2012**, *45*, 837–849. [CrossRef]
12. Gong, Q.M.; Zhou, X.X.; Yin, L.J.; He, G.W.; Miao, C.T. Study of Rock Breaking Efficiency of TBM Disc Cutter Basedon Chips Analysis of Linear Cutting Test. *Tunn. Constr.* **2017**, *37*, 363–368. (In Chinese)
13. Rostami, J.; Özdemir, L. A new model for performance prediction of hard rock TBMs. In Proceedings of the Rapid Excavation and Tunneling Conference, Boston, MA, USA, 13–17 June 1993; pp. 793–809.
14. Hamzaban, M.T.; Memarian, H.; Rostami, J.; Ghasemi-Monfared, H. Study of Rock–Pin Interaction in Cerchar Abrasivity Test. *Int. J. Rock Mech. Min. Sci.* **2014**, *72*, 100–108. [CrossRef]
15. Man, K.; Liu, X.L.; Song, Z.F.; Liu, Z.X.; Liu, R.L.; Wu, L.W.; Cao, Z.X. Dynamic Compression Characteristics and Failure Mechanism of Water-Saturated Granite. *Water* **2022**, *14*, 216. [CrossRef]

16. Mammen, J.; Saydam, S.; Hagan, P. A Study on the Effect of Moisture Content on Rock Cutting Performance. In Proceedings of the 2009 Coal Operators' Conference, University of Wollongong & the Australasian Institute of Mining and Metallurgy, Wollongong, Australia, 12–13 February 2009; pp. 340–347.
17. Bakar, M.Z.A.; Gertsch, L.S. Evaluation of Saturation Effects on Drag Pick Cutting of a Brittle Sandstone from Full Scale Linear Cutting Tests. *Tunn. Undergr. Space Technol.* **2013**, *34*, 124–134. [CrossRef]
18. Mosleh, M.; Gharahbagh, E.A.; Rostami, J. Effects of Relative Hardness and Moisture on Tool Wear in Soil Excavation Operations. *Wear* **2013**, *302*, 1555–1559. [CrossRef]
19. Bakar, M.Z.A.; Gertsch, L.S.; Rostami, J. Evaluation of Fragments from Disc Cutting of Dry and Saturated Sandstone. *Rock Mech. Rock Eng.* **2014**, *47*, 1891–1903. [CrossRef]
20. Zhu, G.X.; He, L.K.; Tan, Q.; Yao, Z.W.; Zhang, Y.C. Experimental study on the rock breaking characteristics of TBM disc cutter under saturated condition. *J. Railw. Sci. Eng.* **2019**, *16*, 3126–3133. (In Chinese) [CrossRef]
21. Yan, C.B.; Gao, Z.A.; Yao, X.T.; Wang, H.J.; Yang, F.W.; Yang, J.H.; Lu, G.M. Weighted random forest prediction model for TBM advance rate considering uncertainty. *Chin. J. Geotech. Eng.* **2023**, *45*, 2575–2583. (In Chinese) [CrossRef]
22. Shen, Y.M.; Zhang, D.M.; Wang, R.L.; Li, J.P.; Huang, Z.K. SBD-K-medoids-based long-term settlement anlysis of shield tunnel. *Transp. Geotech.* **2023**, *42*, 101053. [CrossRef]
23. Rispoli, A.; Ferrero, A.M.; Cardu, M.; Farinetti, A. Determining the Particle Size of Debris from a Tunnel Boring Machine Through Photographic Analysis and Comparison Between Excavation Performance and Rock Mass Properties. *Rock Mech. Rock Eng.* **2017**, *50*, 2805–2816. [CrossRef]
24. Tuncdemir, H.; Bilgin, N.; Copur, H.; Balci, C. Control of Rock Cutting Efficiency by Muck Size. *Int. J. Rock Mech. Min. Sci.* **2008**, *45*, 278–288. [CrossRef]
25. *BS EN 933-1-2012*; Tests for Geometrical Properties of Aggregates. Determination of Particle Size Distribution. Sieving Method. BSI Standards Limited: London, UK, 2012. [CrossRef]
26. *ASTM D7625*; Standard Test Method for Laboratory Determination of Abrasiveness of Rock Using the CERCHAR Method. ASTM International: West Conshohocken, PA, USA, 2010. [CrossRef]
27. Jing, L.J.; Zhang, N.; Yang, C.; Ju, X.Y. A Design Method Research on TBM Face Cutter Spacing Layout Based on Mnimum Specific Energy. *J. China Railw. Soc.* **2018**, *40*, 123–129. (In Chinese) [CrossRef]
28. Roxborough, F.F.; Rispin, A. The mechanical cutting characteristics of the lower chalk. *Tunn. Tunn.* **1973**, *5*, 45–67.
29. Yan, C.B.; Jiang, X.D.; Liu, Z.H.; Yang, J.H.; Miao, D. Rock-breaking efficiency of TBM based on particle-size distribution of rock detritus. *Chin. J. Geotech. Eng.* **2019**, *41*, 466–474. (In Chinese) [CrossRef]
30. Gong, Q.M.; Zhao, J.; Jiang, Y.S. In Situ TBM Penetration Tests and Rock Mass Boreability Analysis in Hard Rock Tunnels. *Tunn. Undergr. Space Technol.* **2007**, *22*, 303–316. [CrossRef]
31. Yan, C.B.; Li, G.L.; Chen, J.; Li, Y.; Yang, Y.D.; Yang, F.W.; Yang, J.H. A novel evaluation index of TBM rock-breaking efficiency based on newly added surfaces theory. *Rock Soil Mech.* **2023**, *44*, 1153–1164. (In Chinese) [CrossRef]
32. Yao, Q.L.; Zhu, L.; Huang, Q.X.; Yang, P.; Xu, Z. Experimental study on the effect of moisture content on creep characteristics of fine-grained feldspar lithic sandstone. *J. Min. Saf. Eng.* **2019**, *36*, 10347–1042+1051. (In Chinese) [CrossRef]
33. Li, T.B.; Chen, Z.Q.; Chen, G.Q.; Ma, C.C.; Tang, O.L.; Wang, M.J. An experimental study of energy mechanism of sandstone with different moisture contents. *Rock Soil Mech.* **2015**, *36*, 229–236. (In Chinese) [CrossRef]
34. Bakar, M.Z.A.; Majeed, Y.; Rostami, J. Effects of Rock Water Content on CERCHAR Abrasivity Index. *Wear* **2016**, *368–369*, 132–145. [CrossRef]